HHS Public Access

Author manuscript

Nanomedicine. Author manuscript; available in PMC 2018 February 14.

Published in final edited form as:

Nanomedicine. 2015 April ; 11(3): 489–498. doi:10.1016/j.nano.2014.09.020.

Antigenic Composition of Single Nano-Sized Extracellular Blood Vesicles

Anush Arakelyan[1], **Oxana Ivanova**[2], **Elena Vasilieva**[2], **Jean-Charles Grivel**[1,*], and **Leonid Margolis**[1,*]

[1]Program in Physical Biology, Eunice Kennedy-Shriver National Institute of Child Health and Human Development, National Institutes of Health, Bethesda, MD, USA

[2]Atherothrombosis Department, Moscow State University of Medicine and Dentistry, Moscow, Russia

Abstract

Extracellular vesicles (EVs) are important in normal physiology and are altered in various pathologies. EVs produced by different cells are antigenically different. Since the majority of EVs are too small for routine flow cytometry, EV composition is studied predominantly in bulk, thus not addressing their antigenic heterogeneity. Here, we describe a nanoparticle-based technique for analyzing antigens on *single* nano-sized EVs. The technique consists of immuno-capturing of EVs with 15-nm magnetic nanoparticles, staining captured EVs with antibodies against their antigens, and separating them from unbound EVs and free antibodies in a magnetic field, followed by flow analysis. This technique allows us to characterize EVs populations according to their antigenic distribution, including minor EV fractions. We demonstrated that the individual blood EVs carry different sets of antigens, none being ubiquitous, and quantified their distribution. The physiological significance of antigenically different EVs and their correlation with different pathologies can now be directly addressed.

Graphical abstract

[*]Correspondence should be addressed to: L.M. (margolis@helix.nih.gov) or J-C.G. (grivelj@mail.nih.gov).

Contribution: A.A. developed the technique, performed the main body of experiments, analyzed data, and revised the manuscript. O.I. performed experiments. E.V. determined antigens to analyze, discussed data, and revised the manuscript. J-C.G. invented and developed the technique, analyzed data, interpreted results, and revised the manuscript. L.M. coordinated the study, interpreted results, and wrote and revised the manuscript.

Conflict-of-interest disclosure: The authors declare no competing financial interests.

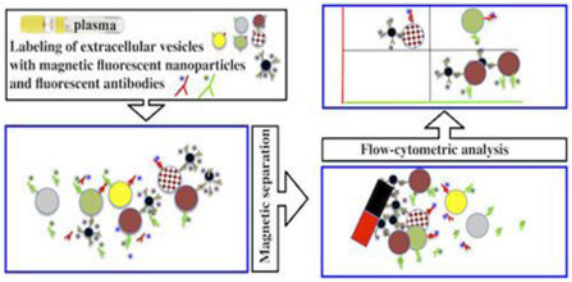

Background

Extracellular vesicles (EVs): microvesicles, exosomes, and apoptotic bodies are released from cells through either direct membrane outward budding or the late endosomal–lysosomal pathway[1,2]. EVs play an important role in cell-to-cell communication because different proteins, lipids and RNAs are specifically incorporated into these vesicles, which can be targeted to remote cells through receptor-ligand interactions[1,3]. Release of EVs was reported to change in pathologies (reviewed in[4,5]) including cancer[6-9], neurological, hematological [9], cardiovascular[10,11], autoimmune and rheumatologic[12] diseases, and viral infection[13-15].

Since various cells supplying EVs express different antigens, EVs produced by these cells are antigenically different. For example, CD81, a member of the tetraspanin superfamily, is expressed on several cell types including hepatocytes and B lymphocytes[16]; CD63, another member of this family, is expressed on activated platelets, endothelium, fibroblasts, and macrophages[17,18]; CD41, an integrin alpha chain 2b, is a heterodimeric integral membrane protein expressed on platelets, megakaryocytes, and hematopoietic stem cells[19]; CD31, a platelet endothelial cell adhesion molecule, is expressed on vascular endothelial cells, platelets, naïve T cells, monocytes, and neutrophils[20].

Analyses of blood EV composition, which have been performed predominantly in bulk, have revealed the presence of various cellular antigens in EVs[21] but could not reflect the distribution of these antigens on individual EVs although such distribution may report on physiological conditions of the donor[22,23].

Conventional flow cytometry cannot be applied to analysis of small particles like EVs. Several attempts to overcome this limitation have been reported, including the use of single nanometric particle enumerators[24], microfluidics-based cytometers[25], and cytometers optimized to improve light scattering collection[26,27]. While these methods have confirmed the diversity of EV size and quantity[28,29], in most cases they failed to address the compositional diversity of EVs.

While EVs can become visible in flow cytometers upon their staining with fluorescent antibodies, it is difficult to distinguish them from free fluorescent antibodies. Recently it was reported that using a BD Influx flow cytometer with wide-angle forward scatter it is possible to visualize small fluorescent particles, including EVs labeled with fluorescent antibodies[30,31].

Here, we report on the analysis of surface proteins on *single* nano-sized (<300 nm) EVs with a newly developed nanoparticle-based technique. We used a commercial flow cytometer and magnetic nanoparticles to isolate fluorescence-labeled EVs and to separate them from non-bound fluorescent antibodies. We demonstrate that the blood EVs are highly heterogeneous in surface proteins, with none of the analyzed antigens being ubiquitous. Our analysis revealed the distribution of several antigens and their combinations on *single* vesicles.

Methods

EV preparation and labeling

Microvesicles derived from the SUPT1-CCR5 CL.30 cell line were purified on sucrose gradients and non-specifically labeled with either Alexa Fluor 488 5C Maleimide (50μM) or Alexa Fluor 633 5C Maleimide (38μM) as described[32] (kindly provided by Dr. J. Lifson).

Normal blood plasma from the NIH blood bank was collected in several 8-ml tubes with sodium citrate (3.2%); the first tube was discarded to avoid collecting EVs released by platelets activated by venipuncture. Collection tubes were centrifuged at 3,000 *g* for 15 min to obtain platelet-poor plasma (PPP), followed by a thromboplastin treatment and by the isolation of EVs as described in the Exoquick protocol.

Alternatively, we used PPP, was enriched with EVs by centrifugation with 100K MWCO (Amicon Millipore, Billerica, MA) concentrators (8-fold enrichment).

Coupling of monoclonal antibodies to magnetic nanoparticles

Carboxyl-terminated magnetic iron oxide nanoparticles (MNPs; 1 mg of 15-nm particles) (Ocean NanoTech, Springdale, AR) were coupled to mouse-anti-human monoclonal antibodies recognizing different EV antigens. The three antibodies used alternatively for coupling to MNPs were anti-CD81 (eBioscience, San Diego, CA), anti-CD63, and anti-CD31 (BioLegend, San Diego, CA), as previously described[33]. Briefly, 1 mg of MNPs was incubated in 200 μl of activation buffer supplemented with 1.7 mM 1-(3-Dimethylaminopropyl)-3-ethylcarbodiimide hydrochloride and 0.76 mM N-hydroxysulfosuccinimide (Sulfo-NHS) for 10 min at room temperature. After activation, 500 μl of coupling buffer was added to the MNPs, followed by the addition of 1 mg of the purified antibody. After a 2-h in a thermo mixer at room temperature, the reaction was stopped with 10 μl of quenching solution, transferred to a 5ml propylene round-bottom tube (12- × 75-mm, BD Falcon) and inserted into SuperMag Separator™ magnetic separator. We performed two washes using a SuperMAG-01 magnetic separator (Ocean NanoTech) at 4°C. The coupled MNPs were suspended in 2 ml of storage buffer and stored at 4°C at a concentration of 0.5 mg/ml of iron oxide (based on the initial iron oxide concentration provided by the manufacturer).

Capture and detection of EVs with nanoparticles

To visualize the anti-EV-antibody-MNP- complexes, MNPs coupled to anti-EV antibody were incubated with 5 μg of Alexa Fluor 488-labeled goat anti-mouse IgG Fab fragments (Zenon anti-mouse IgG, Life Technologies, Carlsbad, CA). To separate free Fab fragments

from the bound ones the preparation was washed twice with 300 μl of PBS on a 100-kD nanosep centrifugal device (Pall Corporation, Port Washington, NY) and recovered in its initial volume.

Next, a 10^6 excess of Zenon-labeled MNPs coupled to an antibody against an EV antigen were incubated with EVs one hour at 4°C. Various combinations of monoclonal antibodies against other cellular antigens on EVs: anti-CD31-PE, anti-CD81-PE (BioLegend, San Diego, CA), and anti-CD41-APC (BD, Pharmigen, San Diego, CA) were added for 15 min at room temperature.

EV–MNPs–antibodies complexes were separated on μMACS magnetic columns (Miltenyi Biotech, Auburn, CA) in a high magnetic field generated by a OctoMacs magnet (Miltenyi Biotech). The columns were washed three times with a washing buffer consisting of PBS, 0.5% BSA, and 2 mM EDTA; the complexes were eluted off the magnet in 2×200 μl of PBS and fixed in 1% formaldehyde in PBS. To evaluate the efficiency of separation of unbound antibodies, to EV-MNPs complexes, we added fluorescent isotype control antibodies (which should not bind to EVs), and acquired this mixture on the flow cytometer and compared with the same preparation subjected to a magnetic column separation. There was less than 1% of non-specific fluorescent antibodies co-purified with the EVs (Figure S1).

Separated MNPs-EV complexes were subjected to flow analysis. AccuCheck beads (50μl; Life Technologies) were added to each elution tube to evaluate the volume acquired for flow analysis. On the basis of this volumetric measurement, the number of events can be recalculated as EV concentrations.

iMFI, which reports on the integrated fluorescence intensity by combining the relative amount of positive events with the mean fluorescence intensity (MFI) of these events[34,35] was calculated as suggested iMFI= (MFI) × (P); where P is the fraction of positive events.

We used LSRII (BD Biosciences, San Jose, CA) flow cytometer equipped with 355-, 407-, 488-, 532- and 638- nm laser lines.

Compensation beads (BD) were used to perform compensation controls.

Detection of EVs by ELISA

Nunc MAXISORP plates (Nalgene- Nunc, Penfield, New York, USA) were coated with 50μl of a 4μg/ml solution of anti-CD81 antibody (clone 5A6, BioLegend) in PBS. The plate was washed and blocked overnight with 100μl of antibody/Antigen Conjugate Diluent/Blocker (Poly-HRP) (Fitzgerald Industries International, Acton, MA) and washed with PBS. EVs were purified with Exoquick from 500 μl of PPP. Aliquots of these EVs were treated with anti-CD81 MNPs and separated on a magnetic column. The flow-through fraction was diluted three times in PBS and incubated in duplicate wells in the coated plate. A remaining aliquot, representing the EVs input was diluted three times in PBS and incubated in duplicate wells of the coated ELISA plate. Following a one–hour incubation, the plate was washed with PBS and incubated with 50μl of biotinylated anti-CD81 antibody at a 1μg/ml. The plate was washed with PBS and incubated with 50μl of 0.2 μg/ml solution of Poly-HRP 20 (Fitzgerald Industries International). Following four washes, the plate was incubated with

50 μl of TMB (Fitzgerald Industries International) for 20 minutes and read at 367 nm with a Tecan Safire II (Tecan, Austria) using Magelan 6.0.

Results are reported as optical density at 367 nm.

Statistical analysis

Descriptive statistics were calculated with Excel. Comparisons of the proportions of captured EVs, either pre-labeled or not, were performed with a χ^2 test using JMP 9.0 (SAS Institute, Cary, NC). The results are presented as means ± standard errors of the mean (SEM), and *n*, the number of replicates, is indicated. CV, the coefficient of variation, was calculated by expressing the standard deviation as % of the mean. The numbers of EVs captured at different MNP-to-EV ratios were modeled using JMP software. The Gompertz 3P sigmoid curve gave the best data fit and was used to estimate the optimal ratio by inverse prediction function.

Results

For analysis of individual EVs we (i) coupled magnetic nanoparticles (MNPs) to mouse anti-human antibodies against EV surface antigens, (ii) stained MNPs with fluorescent anti-mouse IgG1 Fab fragments, (iii) captured EVs with antibody-coupled MNPs, (iv) stained the resultant complexes with fluorescent “detection” antibodies against antigens of interest, (v) separated EV-MNP-detection antibody complexes from free antibodies in a strong magnetic field using magnetic columns, and (vi) analyzed complexes with a flow cytometer set to be triggered by fluorescence, rather than by light scattering.

We first analyzed individual EVs in a reductionist model of cloned cells releasing vesicles into the culture medium and then studied the distribution of individual EVs in the blood of healthy individuals.

Flow analysis of SUPT1-CCR5CL.30 cell line-generated EVs

First, we investigated whether the EVs captured by antibody-coupled MNPs and detected as events in flow analysis represent individual vesicles. We divided EV preparations into two fractions, one labeled with Alexa Fluor 488 and the other with Alexa Fluor 633; combined these two differentially labeled EVs in equal quantities; incubated them with MNPs coupled to anti-CD81 antibodies (a common EV antigen[21]); separated captured EVs in a magnetic field and analyzed them using a flow cytometer. EV aggregates bound to MNPs should appear as events positive for both fluorophores. On average, only 9.6%±0.5% (n =4) of events represented EV aggregates. Thus, about 90% of MNP-bound EVs observed in flow analysis represent single vesicles (Figure 1). This is in stark contrast with results from large 4.5μm Exosome Dynabeads®, which bind multiple EVs that can only be further analyzed collectively (see Figure S2).

Next, we determined the MNP-to-EV ratio that maximizes EV capture, using anti-CD81 capture MNPs at concentrations varying from 34×10^7/μl to 34×10^9/μl and Alexa Fluor 633-labeled EVs at concentrations varying from 18×10^3/μl to 87×10^5/μl. For each experiment performed at a given MNP-to-EV ratio, we purified the complexes on a magnetic column

and enumerated these labeled EVs both in the fraction that was retained on the magnetic column and in the fraction that was not (flow-through). We found that, at different ratios of MNPs to EVs, these fractions vary, and at a ratio above 2.3×10^5 (as evaluted with a regression curve (Figure S3)), we capture 95% of EVs towards which MNPs are targeted. In our experiments presented below we typically used MNPs at the ratio to EVs higher than 106 capturing essentially all the EVs of interest.

To evaluate the efficiency of the assay, using volumetric controlled flow analysis, we enumerated labeled EVs in the initial preparation, in the fractions of EVs captured with anti-CD81, and in the flow-through. The latter were subjected to another capture procedure. We captured almost all CD81-carrying EVs present in the preparation, since a second capture procedure of the flow-through fraction of EVs with anti-CD81 MNPs resulted in recapture of less than 1% (Figure 2A, B) of the original EVs. To confirm this high capture efficiency, we evaluated with ELISA the amounts of CD81 in the initial preparation of EVs isolated from blood plasma and in the flow-through fraction after capturing EVs with anti-CD81 MNPs. In this assay, less than 6% of the initial amount of CD81 was revealed in the flow through-fraction (Figure 2C).

Flow analysis of EVs isolated from blood plasma

Empowered by the results of analysis of EVs in cell culture supernatant, we analyzed single EVs in blood plasma. EVs were isolated with Exoquick, captured with MNPs, stained with detection antibodies, and purified in a magnetic field. We added AccuCheck beads to estimate the sample volume acquired in order to accurately determine EV concentrations. The total number EVs in our plasma was ~3,500 per μl, as evaluated for plasma samples in which EVs were stained with the fluorescent lipidic dye DiI (data not shown). This number is within the earlier reported range (see [22,23]), although it varies between plasmas from different donors.

We further analyzed the composition of plasma EVs by capturing them with MNPs coupled to antibodies recognizing EVs-specific antigens and staining them with detection antibodies. The specificity of the capture of plasma EVs with MNPs coupled to EVs-specific antibodies was demonstrated by comparison with MNPs coupled to non-specific control antibodies (Figure 3A,B). This specificity of capture is reflected in the integrated MFI (iMFI)[34,35], which combines the relative amount of positive events with the mean fluorescence intensity of these events: 5574 and 70 for CD81, and 2074 and 22 for CD41 for specific staining and isotype control, respectively. Also, we used isotype control antibody to verify the specificity of detection of EV antigens (Figure 3D,F). Using this approach, we demonstrated that the fraction of captured EVs depended on the capture-antigen and for CD81 constituted about 30% of total EVs, while CD31/CD81 and CD31/CD41 EVs represented smaller fractions (Figure 3C,E). The specific capture of EVs by MNPs allowed us to focus on relatively small fractions of EVs, in particular on EVs carrying CD31. At first, we tried to identify these EVs in the large pool of vesicles that express CD81, which was defined earlier as one of the prevalent EV antigens [21]. However, when we stained these vesicles for CD31, their numbers were only slightly above the isotype control and not significantly different from it (5±2 EVs/μl for specific staining for CD81+CD31+ EVs vs. 2.7±1.2/μl isotype control staining, n=4,

p=0.3). In contrast, when we first captured CD31-expressing EVs with anti-CD31 MNPs, and stained them for CD81 we reliably identified CD81 co-expressing EVs, which were present on average at a concentration of 101± 32/μl (n=4), which is significantly higher than when EVs were stained with an isotype control antibody (2.3±1.5/μl, p= 0.03) (Figure 3C, D. iMFI 6451 and 104 for c and d, respectively).

We further analyzed CD31-carrying EVs for expression of CD41. On average, per microliter there were 80±27 CD31-captured EVs that expressed CD41 (n=5). In isotype control, on average there were 3.2±1.0 positive events/μl (n=5) (Figure 3E,F, iMFI 2070 and 107 for e and f, respectively). To test whether bound MNPs can shield other EV surface antigens by steric hindrance, we compared the amount of EVs when we first captured EVs with anti-CD31 MNPs and then stained with anti-CD41 antibodies (Figure 4A,B) with the amount detected when we first stained EVs with anti-CD41 antibodies and then captured them with anti-CD31 MNPs (Figure 4C,D). The results were similar (p=0.12), suggesting that MNPs bound to CD31 do not shield this EV antigen. Also, similar concentrations of EVs were evaluated when we either captured them with anti-CD63 MNPs and then stained with anti-CD41 antibodies or first stained with anti-CD41 antibodies and then captured with anti-CD63 MNPs (data not shown).

To analyze the fine distribution of CD31-carrying EVs, we stained them with both anti-CD41 and anti-CD63 detection antibodies. Among CD31-captured EVs that expressed CD41, on average 80.6%±5.7% were positive for CD63 (n=7), while among CD31-captured EVs that expressed CD63, on average 41%±5.8% (n=7) co-expressed CD41. The absolute amounts of these EVs were donor-dependent: in samples from different donors the concentrations of CD31+CD41+ EVs in plasma varied between 24/μl and 170/μl.

Flow analysis of EVs in blood plasma

The data presented in the previous section were obtained on EVs isolated with Exoquick. Although this is a widely used method for EV isolation[36], we decided to modify our protocol to exclude this isolation step and to analyze individual EVs directly from blood plasma.

Platelet poor plasma (PPP) was incubated with MNPs coupled to antibodies against EV surface antigens. Figure 5 illustrates the result of such analysis with EVs captured with anti-CD63 MNPs and stained for CD41. 0.1 ml of 8-fold concentrated PPP was enough to capture EVs that carry CD41 (Figure 5A) in amounts that were far in excess of non-specific events (Figure 5B). To estimate the reproducibility of our analysis and of the variability between different donors, we performed this assay on samples from two donors, each in triplicate. In this analysis, the concentration of CD63-captured CD41-positive EVs was 87±6/μl in one patient and 26±2/μl in another patient (CVs 12.1% and 13.2%, respectively). Thus, our assay can directly capture EVs from plasma and is reproducible at both low and high EV counts.

Discussion

The physiological role of the vesiculation of cell membranes was emphasized about 30 years ago[37,38]. However, it is only recently that cell-derived EVs have attracted much attention, since it is now understood that EVs generation is a normal physiological process involved in cell–cell communications[39,40]. Although EVs have been found in all body fluids, the exact functional difference between various EVs has not been yet established.

Recently, it was reported that blood EV spectra are changed in various diseases, in particular in cardiovascular disease. For example, it was reported[22,23] that EV shedding is increased with the exacerbation of cardiovascular disease, but not with the atherosclerotic burden in stable patients. These and other reports[41,42] attracted attention to the association of blood EVs with particular medical conditions.

Until recently, studies were focused on EVs of 0.5 to 1μm in diameter, which were studied predominantly with flow cytometry developed for cells. However, recent analysis of EVs with high-resolution atomic force microscopy revealed that vesicles of such size constitute only a small percentage of the total EV population. The rest of the EVs are of approximately 100 nm[43] and thus are too small to be visible with regular light microscopy or to be detected with routine flow cytometry.

Unfortunately, contemporary methods predominantly analyze EVs in bulk. Such an approach ignores the importance of particular fractions of EVs by diluting the sought-after specific signal in the noise of the overall output. These bulk methods include biochemical analysis of EV extracts as well as immunochemical analysis of EVs adsorbed on various particles. In particular, a method of adsorbing EVs on microbeads, such as Exosome Dynabeads® followed by staining with fluorescent antibodies and analysis with flow cytometer, has been described[44]. However, numerous EVs are attached to each microbead, and this method thus constitutes essentially another bulk analysis. Such analyses have helped identifying antigens in EV preparations but have failed to analyze their presence on individual EVs, as confirmed in the present work (Figure S2).

Most of the methods used to monitor and analyze individual EVs have been restricted to the evaluation of the number and physical parameters of individual EVs and have included atomic force microscopy, dynamic light scattering, nanoparticle tracking analysis, evaluation of particle ζ-potential, as well as other methods[45]. While these methods establish the heterogeneity of individual EVs, new high-throughput methods are necessary to characterize the composition of individual EVs as flow cytometry did for individual cell analysis.

The diversity of molecules carried by EVs stems from the fact that they are shed into blood by diverse cells. Using EVs as biomarkers reflecting the origin and physiological status of the producing cells in norm and in diseases requires distinguishing EV subpopulations on the basis of their individual cellular markers against the background of the output of all cells irrelevant to the phenomenon studied.

Here, we analyzed the antigenic make-up of single EVs and quantified diverse subpopulations of EVs according to the antigens they carry. In contrast to most published

data, we focused our analysis on small EVs below 300 nm, which constitute the vast majority of blood EVs[43] and which because of their small size cannot be analyzed with routine flow cytometry.

Our analysis is based on using 15-nm MNPs, which, through a “capture” antibody against EV surface protein, bind to EVs. In these complexes of single EVs bound to magnetic nanoparticles, various EVs antigens can be revealed with specific fluorescent antibodies. The magnetic properties of the complexes allow us to separate them from unbound antibodies in a magnetic field, thus excluding the background fluorescence “noise” these antibodies generate. Earlier, we applied MNPs to the analysis of individual HIV-1 virions[33].

Separation of EVs in a high-energy magnetic field using the magnetic properties of MNPs that capture them is crucial since, unlike conventional cellular analysis in which the washing of free-floating antibodies can be skipped by use of a proper FSC threshold, the inability of conventional cytometers to detect the light scattering of sub-microscopic vesicles does not allow the distinction between vesicle-bound and free antibodies. In the absence of separation from free antibodies, fluorescent EVs would be lost in a sea of antibodies and their aggregates (Figure S1). Use of MNPs allows the complete separation of EVs carrying a particular antigen from non-bound fluorescent antibodies within 10 min, while separation in sucrose gradients requires a 14- to 20-h centrifugation[30,31].

Although, with magnetic columns we efficiently separated MNPs-EV complexes bound to fluorescent detection antibodies from unbound antibodies, we did not rely exclusively on the purity of the final preparation but applied an additional marker to exclude unbound antibodies: we labeled MNPs with fluorescent Fab against the capture antibody, thus introducing another fluorescent molecule into the MNPs-EV complexes. The antibody-EV-MNPs complexes are then identified on the basis of their positivity for at least two fluorescent markers, while free antibodies are not visualized even if they had contaminated the final preparation.

Another important part is the flow cytometer setting. For cell analysis, these instruments are set to trigger on the light scattered when a cell crosses the laser beam. EV-MNPs complexes are too small to trigger a flow cytometer with light scattering, so the trigger event has to be set on a fluorescence channel.

CD81 has been reported to be common for certain types for EVs[21], and we used this antigen to capture EVs generated by lymphocytic cells in culture. We found that to maximize EV capture, we need more than five-order excess of MNPs. At the MNP-to-EV ratio of 10^6 used in our experiment, about 99% of EVs bind to MNPs and are retained in the magnetic field. As with the immune staining of cells when antibodies are added in vast excess but only a small fraction actually binds to their antigens, the majority of MNPs does not bind to EVs but remains free. These MNPs do not interfere with the analysis of MNPs–EV complexes, which unlike free MNPs carry several fluorophores. As far as the EV-bound MNPs are concerned, they do not seem to be a steric hindrance preventing free antibodies from binding to their antigens. Indeed, reversing the order of EV capture with MNPs and staining with a detection antibody did not significantly affect the estimated quantity of EVs.

To prove that the recorded events predominantly represent individual EVs, we labeled EVs with two different fluorophores, mixed these two fractions, and captured them with anti-CD81 MNPs. Aggregates of EVs would predominantly be seen as events positive for both fluorophores. Such events represented a small fraction of the total, whereas about 90% of the events reflected individual EVs. Thus, unlike most of the other EVs studies that characterize them in bulk, here we analyzed the antigenic composition of *individual* cell-derived and blood-derived EVs and quantitated their diversity.

We found that although CD81 is a common antigen, it is not ubiquitous: it is associated with less than 30% of blood EVs. These numbers reflect the true presence of CD81-carrying EVs in the preparation, rather than the efficiency of capture. Indeed, recapture of the EVs that were not captured in the first run revealed that we might have missed less than 1% of CD81-carrying EVs. The high efficiency of capture was confirmed when we evaluated the non-captured CD81-carrying EVs with ELISA. Thus, EVs show a large degree of heterogeneity, not only when they are derived from different cell types as found in plasma, but also when they are derived from cloned cells; a result that could not be obtained from a bulk analysis of EVs.

While it may seem possible to capture the majority of EVs through a highly prevalent antigen such as CD81, minor fractions of CD81-carrying EVs, e.g., CD31-bearing, are difficult to identify because of a low signal-to-noise ratio. In particular, when we focused on CD31-carrying blood EVs among CD81-captured EVs, these EVs were barely above the non-specific background. In contrast, when we used anti-CD31 MNPs we reliably identified them, visualizing CD81 on their surfaces as well as CD63 and CD41. We reliably detected ~5 EVs per microliter of concentrated plasma. To what concentration of EVs in the original sample this number corresponds depends on how much the original sample was concentrated. In our experiments we concentrated 5 to 8 times.

Unlike most published EV analyses, here we not only registered the diversity of EVs in their expression of different antigens but also quantified their distribution. Moreover, this analysis can be performed not only on EVs released by cells in culture, but also directly on blood plasma EVs. With MNPs coupled to antibodies against EV antigens, it is possible to focus on EVs that constitute a small fraction of EVs present in normal blood plasma. Moreover, we were able to evaluate the distribution of other antigens in these minor EV fractions. In particular, when we captured CD31-carrying EVs, we found that about half of these EVs co-expressed CD41 and CD63. Although CD63 is a highly prevalent antigen, our fine analysis of antigen distribution demonstrated that within the sensitivity limit of our cytometer, it is not carried by approximately 20% of the CD31+CD41+ EVs; thus these EVs form a separate fraction.

In conclusion, here we performed a fine analysis of single blood EVs according to the distribution of their antigens. We demonstrated that the blood EV population is a mosaic, with various EVs carrying different combinations of antigens. None of these antigens can be claimed to be present on all EVs. These results would be impossible to obtain in a bulk analysis, which reports only on the general presence of particular antigens in EV preparations. Moreover, since many of the plasma membrane antigens are common to more

than one cell type, individual EVs should be characterized by combinations rather than by single antigens.

Because of the reproducibility of our analysis of distributions of individual blood EVs according to the combinations of antigens they carry, it is now possible to relate these distributions to the medical condition of an individual donor, as well as to search for EV antigenic patterns common to particular diseases. The physiological significance of antigenically different individual EVs and their correlation with different pathologies can now be directly addressed.

Supplementary Material

Refer to Web version on PubMed Central for supplementary material.

Acknowledgments

Funding: The work of A.A., J-C.G, and L.M. was supported by the Intramural NICHD Program. The work of E.V. and O. I. was supported by Russian Federation Government grant “Immunovirology of atherosclerosis” #14.B25.31.0016.

References

1. Thery C, Ostrowski M, Segura E. Membrane vesicles as conveyors of immune responses. Nat Rev Immunol. 2009; 9(8):581–593. Prepublished on 2009/06/06 as. DOI: 10.1038/nri2567 [PubMed: 19498381]
2. Kalra H, Simpson RJ, Ji H, et al. Vesiclepedia: a compendium for extracellular vesicles with continuous community annotation. PLoS Biol. 2012; 10(12):e1001450. Prepublished on 2012/12/29 as. doi: 10.1371/journal.pbio.1001450 [PubMed: 23271954]
3. Cocucci E, Racchetti G, Meldolesi J. Shedding microvesicles: artefacts no more. Trends Cell Biol. 2009; 19(2):43–51. Prepublished on 2009/01/16 as. DOI: 10.1016/j.tcb.2008.11.003 [PubMed: 19144520]
4. Piccin A, Murphy WG, Smith OP. Circulating microparticles: pathophysiology and clinical implications. Blood Rev. 2007; 21(3):157–171. Prepublished on 2006/11/23 as. DOI: 10.1016/j.blre.2006.09.001 [PubMed: 17118501]
5. Burger D, Schock S, Thompson C, Montezano A, Hakim A, Touyz R. Microparticles: biomarkers and beyond. Clinical science (London, England : 1979). 2013; 124(7):423–441. 10.1042/cs20120309.
6. Taylor DD, Gercel-Taylor C. Exosomes/microvesicles: mediators of cancer-associated immunosuppressive microenvironments. Semin Immunopathol. 2011; 33(5):441–454. Prepublished on 2011/06/21 as. DOI: 10.1007/s00281-010-0234-8 [PubMed: 21688197]
7. Rabinowits G, Gercel-Taylor C, Day JM, Taylor DD, Kloecker GH. Exosomal microRNA: a diagnostic marker for lung cancer. Clin Lung Cancer. 2009; 10(1):42–46. Prepublished on 2009/03/18 as. DOI: 10.3816/CLC.2009.n.006 [PubMed: 19289371]
8. Taylor DD, Gercel-Taylor C. Tumour-derived exosomes and their role in cancer-associated T-cell signalling defects. Br J Cancer. 2005; 92(2):305–311. Prepublished on 2005/01/19 as. DOI: 10.1038/sj.bjc.6602316 [PubMed: 15655551]
9. Toth B, Liebhardt S, Steinig K, et al. Platelet-derived microparticles and coagulation activation in breast cancer patients. Thromb Haemost. 2008; 100(4):663–669. Prepublished on 2008/10/09 as DOI. [PubMed: 18841290]
10. Bernal-Mizrachi L, Jy W, Jimenez JJ, et al. High levels of circulating endothelial microparticles in patients with acute coronary syndromes. Am Heart J. 2003; 145(6):962–970. Prepublished on 2003/06/11 as. DOI: 10.1016/S0002-8703(03)00103-0 [PubMed: 12796750]

11. Xiong J, Miller VM, Li Y, Jayachandran M. Microvesicles at the crossroads between infection and cardiovascular diseases. J Cardiovasc Pharmacol. 2012; 59(2):124–132. Prepublished on 2011/01/19 as. DOI: 10.1097/FJC.0b013e31820c6254 [PubMed: 21242813]
12. Sellam J, Proulle V, Jungel A, et al. Increased levels of circulating microparticles in primary Sjogren's syndrome, systemic lupus erythematosus and rheumatoid arthritis and relation with disease activity. Arthritis Res Ther. 2009; 11(5):R156. Prepublished on 2009/10/17 as. doi: 10.1186/ar2833 [PubMed: 19832990]
13. Dreux M, Garaigorta U, Boyd B, et al. Short-range exosomal transfer of viral RNA from infected cells to plasmacytoid dendritic cells triggers innate immunity. Cell Host Microbe. 2012; 12(4): 558–570. Prepublished on 2012/10/23 as. DOI: 10.1016/j.chom.2012.08.010 [PubMed: 23084922]
14. Rozmyslowicz T, Majka M, Kijowski J, et al. Platelet- and megakaryocyte-derived microparticles transfer CXCR4 receptor to CXCR4-null cells and make them susceptible to infection by X4-HIV. AIDS. 2003; 17(1):33–42. Prepublished on 2002/12/13 as. DOI: 10.1097/01.aids.0000042948.95433.3d [PubMed: 12478067]
15. Bhattarai N, McLinden JH, Xiang J, Landay AL, Chivero ET, Stapleton JT. GB virus C particles inhibit T cell activation via envelope E2 protein-mediated inhibition of TCR signaling. Journal of immunology. 2013; 190(12):6351–6359. Prepublished on 2013/05/21 as. DOI: 10.4049/jimmunol.1300589
16. Pileri P, Uematsu Y, Campagnoli S, et al. Binding of hepatitis C virus to CD81. Science. 1998; 282(5390):938–941. Prepublished on 1998/10/30 as DOI. [PubMed: 9794763]
17. Hamamoto K, Ohga S, Nomura S, Yasunaga K. Cellular distribution of CD63 antigen in platelets and in three megakaryocytic cell lines. Histochem J. 1994; 26(4):367–375. Prepublished on 1994/04/01 as DOI. [PubMed: 8040009]
18. Schroder J, Lullmann-Rauch R, Himmerkus N, et al. Deficiency of the tetraspanin CD63 associated with kidney pathology but normal lysosomal function. Mol Cell Biol. 2009; 29(4): 1083–1094. Prepublished on 2008/12/17 as. DOI: 10.1128/MCB.01163-08 [PubMed: 19075008]
19. Gekas C, Graf T. CD41 expression marks myeloid-biased adult hematopoietic stem cells and increases with age. Blood. 2013; 121(22):4463–4472. Prepublished on 2013/04/09 as. DOI: 10.1182/blood-2012-09-457929 [PubMed: 23564910]
20. Piali L, Hammel P, Uherek C, et al. CD31/PECAM-1 is a ligand for alpha v beta 3 integrin involved in adhesion of leukocytes to endothelium. J Cell Biol. 1995; 130(2):451–460. Prepublished on 1995/07/01 as DOI. [PubMed: 7542249]
21. Escola JM, Kleijmeer MJ, Stoorvogel W, Griffith JM, Yoshie O, Geuze HJ. Selective enrichment of tetraspan proteins on the internal vesicles of multivesicular endosomes and on exosomes secreted by human B-lymphocytes. The Journal of biological chemistry. 1998; 273(32):20121–20127. Prepublished on 1998/08/01 as DOI. [PubMed: 9685355]
22. Porto I, Biasucci LM, De Maria GL, et al. Intracoronary microparticles and microvascular obstruction in patients with ST elevation myocardial infarction undergoing primary percutaneous intervention. Eur Heart J. 2012; 33(23):2928–2938. Prepublished on 2012/03/29 as. DOI: 10.1093/eurheartj/ehs065 [PubMed: 22453653]
23. Biasucci LM, Porto I, Di Vito L, et al. Differences in microparticle release in patients with acute coronary syndrome and stable angina. Circ J. 2012; 76(9):2174–2182. Prepublished on 2012/06/06 as DOI. [PubMed: 22664782]
24. Ferris MM, McCabe MO, Doan LG, Rowlen KL. Rapid enumeration of respiratory viruses. Anal Chem. 2002; 74(8):1849–1856. Prepublished on 2002/05/03 as DOI. [PubMed: 11985317]
25. Huh D, Gu W, Kamotani Y, Grotberg JB, Takayama S. Microfluidics for flow cytometric analysis of cells and particles. Physiol Meas. 2005; 26(3):R73–98. Prepublished on 2005/03/31 as. DOI: 10.1088/0967-3334/26/3/R02 [PubMed: 15798290]
26. Steen HB. Flow cytometer for measurement of the light scattering of viral and other submicroscopic particles. Cytometry Part A : the journal of the International Society for Analytical Cytology. 2004; 57(2):94–99. Prepublished on 2004/01/30 as. DOI: 10.1002/cyto.a.10115 [PubMed: 14750130]

27. Stoffel CL, Kathy RF, Rowlen KL. Design and characterization of a compact dual channel virus counter. Cytometry Part A : the journal of the International Society for Analytical Cytology. 2005; 65(2):140–147. Prepublished on 2005/04/15 as. DOI: 10.1002/cyto.a.20145 [PubMed: 15830378]
28. Robert S, Poncelet P, Lacroix R, et al. Standardization of platelet-derived microparticle counting using calibrated beads and a Cytomics FC500 routine flow cytometer: a first step towards multicenter studies? J Thromb Haemost. 2009; 7(1):190–197. Prepublished on 2008/11/06 as. DOI: 10.1111/j.1538-7836.2008.03200.x [PubMed: 18983485]
29. Lacroix R, Judicone C, Mooberry M, Boucekine M, Key NS, Dignat-George F. Standardization of pre-analytical variables in plasma microparticle determination: results of the International Society on Thrombosis and Haemostasis SSC Collaborative workshop. J Thromb Haemost. 2013; Prepublished on 2013/04/05 as. doi: 10.1111/jth.12207
30. van der Vlist EJ, Nolte-'t Hoen EN, Stoorvogel W, Arkesteijn GJ, Wauben MH. Fluorescent labeling of nano-sized vesicles released by cells and subsequent quantitative and qualitative analysis by high-resolution flow cytometry. Nat Protoc. 2012; 7(7):1311–1326. Prepublished on 2012/06/23 as. DOI: 10.1038/nprot.2012.065 [PubMed: 22722367]
31. Hoen EN, van der Vlist EJ, Aalberts M, et al. Quantitative and qualitative flow cytometric analysis of nanosized cell-derived membrane vesicles. Nanomedicine. 2012; 8(5):712–720. Prepublished on 2011/10/26 as. DOI: 10.1016/j.nano.2011.09.006 [PubMed: 22024193]
32. Morcock DR, Thomas JA, Gagliardi TD, et al. Elimination of retroviral infectivity by N-ethylmaleimide with preservation of functional envelope glycoproteins. Journal of virology. 2005; 79(3):1533–1542. Prepublished on 2005/01/15 as. DOI: 10.1128/JVI.79.3.1533-1542.2005 [PubMed: 15650179]
33. Arakelyan A, Fitzgerald W, Margolis L, Grivel JC. Nanoparticle-based flow virometry for the analysis of individual virions. J Clin Invest. 2013; 123(9):3716–3727. Prepublished on 2013/08/09 as. DOI: 10.1172/JCI67042 [PubMed: 23925291]
34. Darrah PA, Patel DT, De Luca PM, et al. Multifunctional TH1 cells define a correlate of vaccine-mediated protection against Leishmania major. Nature medicine. 2007; 13(7):843–850. Prepublished on 2007/06/15 as. DOI: 10.1038/nm1592
35. Shooshtari P, Fortuno ES 3rd, Blimkie D, et al. Correlation analysis of intracellular and secreted cytokines via the generalized integrated mean fluorescence intensity. Cytometry Part A : the journal of the International Society for Analytical Cytology. 2010; 77(9):873–880. Prepublished on 2010/07/16 as. DOI: 10.1002/cyto.a.20943 [PubMed: 20629196]
36. Taylor DD, Zacharias W, Gercel-Taylor C. Exosome isolation for proteomic analyses and RNA profiling. Methods Mol Biol. 2011; 728:235–246. Prepublished on 2011/04/07 as. DOI: 10.1007/978-1-61779-068-3_15 [PubMed: 21468952]
37. Bastida E, Ordinas A, Escolar G, Jamieson GA. Tissue factor in microvesicles shed from U87MG human glioblastoma cells induces coagulation, platelet aggregation, and thrombogenesis. Blood. 1984; 64(1):177–184. Prepublished on 1984/07/01 as DOI. [PubMed: 6733271]
38. Trams EG, Lauter CJ, Salem N Jr, Heine U. Exfoliation of membrane ecto-enzymes in the form of micro-vesicles. Biochim Biophys Acta. 1981; 645(1):63–70. Prepublished on 1981/07/06 as DOI. [PubMed: 6266476]
39. Valadi H, Ekstrom K, Bossios A, Sjostrand M, Lee JJ, Lotvall JO. Exosome-mediated transfer of mRNAs and microRNAs is a novel mechanism of genetic exchange between cells. Nat Cell Biol. 2007; 9(6):654–659. Prepublished on 2007/05/09 as. DOI: 10.1038/ncb1596 [PubMed: 17486113]
40. Ratajczak J, Wysoczynski M, Hayek F, Janowska-Wieczorek A, Ratajczak MZ. Membrane-derived microvesicles: important and underappreciated mediators of cell-to-cell communication. Leukemia. 2006; 20(9):1487–1495. Prepublished on 2006/06/23 as. DOI: 10.1038/sj.leu.2404296 [PubMed: 16791265]
41. Martinez MC, Tual-Chalot S, Leonetti D, Andriantsitohaina R. Microparticles: targets and tools in cardiovascular disease. Trends Pharmacol Sci. 2011; 32(11):659–665. Prepublished on 2011/07/29 as. DOI: 10.1016/j.tips.2011.06.005 [PubMed: 21794929]
42. Lacroix R, Plawinski L, Robert S, et al. Leukocyte- and endothelial-derived microparticles: a circulating source for fibrinolysis. Haematologica. 2012; 97(12):1864–1872. Prepublished on 2012/06/27 as. DOI: 10.3324/haematol.2012.066167 [PubMed: 22733025]

43. Yuana Y, Oosterkamp TH, Bahatyrova S, et al. Atomic force microscopy: a novel approach to the detection of nanosized blood microparticles. J Thromb Haemost. 2010; 8(2):315–323. Prepublished on 2009/10/21 as. DOI: 10.1111/j.1538-7836.2009.03654.x [PubMed: 19840362]

44. Clayton A, Court J, Navabi H, et al. Analysis of antigen presenting cell derived exosomes, based on immuno-magnetic isolation and flow cytometry. Journal of immunological methods. 2001; 247(1-2):163–174. Prepublished on 2001/01/11 as DOI. [PubMed: 11150547]

45. Müller G. Novel Tools for the Study of Cell Type-Specific Exosomes and Microvesicles. Journal of Bioanalysis & Biomedicine. 2012; 4:46–60. Prepublished on July 25, 2012 as. DOI: 10.4172/1948-593X.1000063

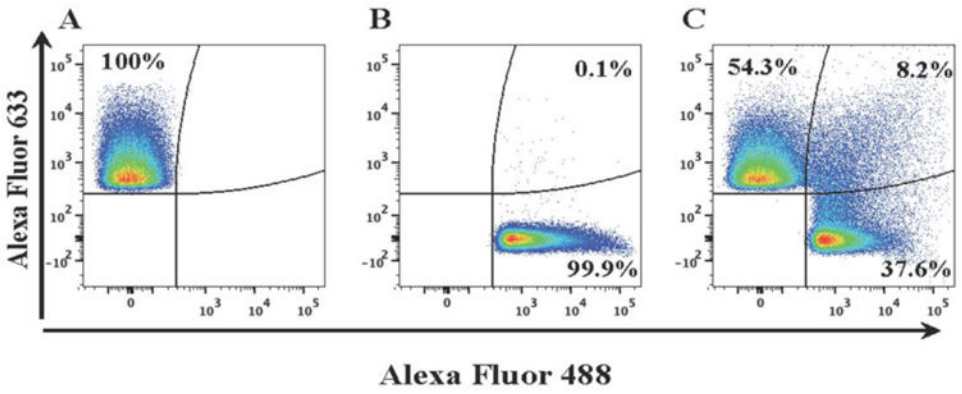

Figure 1. Detection of single EVs

Isolated EVs from SUPT1-CCR5 CL.30 cells were divided into two fractions, one labeled with Alexa Fluor 633 (**A**) and the other with Alexa Fluor 488 (**B**). These fractions were mixed, captured with anti-CD81 MNPs (**C**), and analyzed with flow cytometer. Aggregates were visualized as dual-color events. Note that only about 8% of events represent aggregates. A representative experiment out of four is shown.

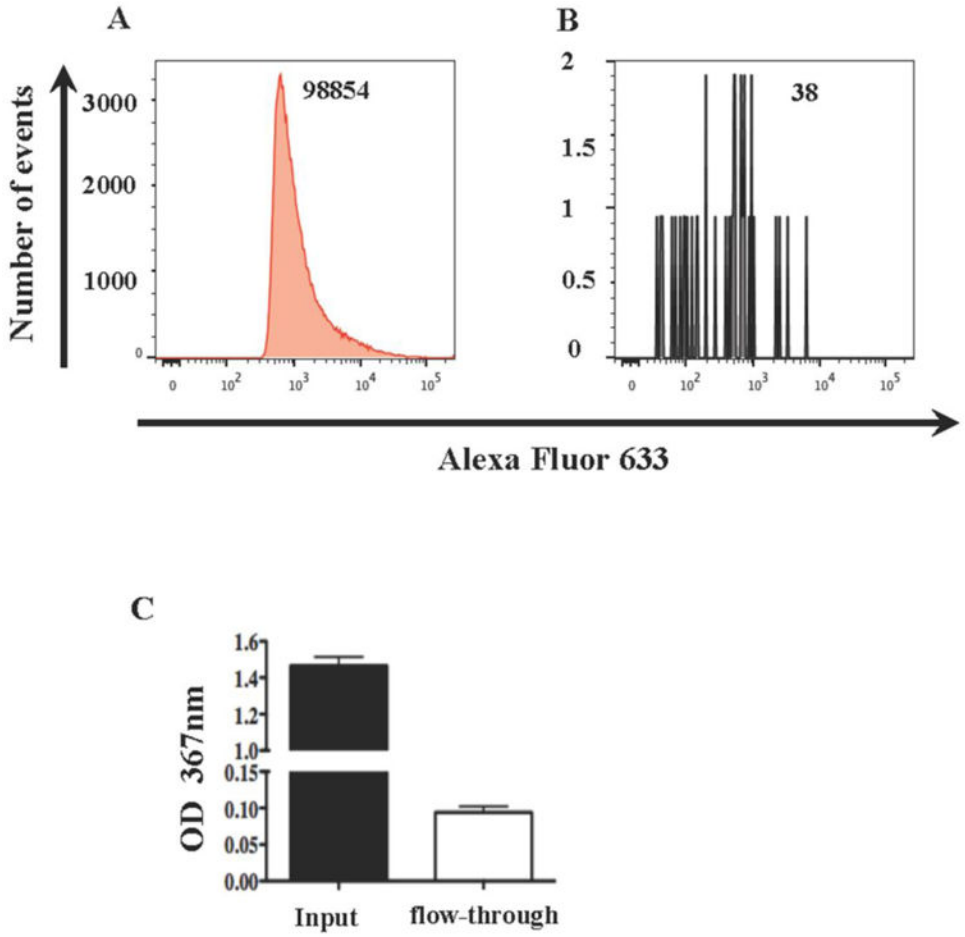

Figure 2. Efficiency of the MNP capture assay

Alexa Fluor 633-labeled EVs isolated from SUPT1-CCR5 CL.30 cells (**A, B**) or blood plasma EVs (**C**) were captured with anti-CD81 MNPs and isolated on a magnetic column. The non-captured (flow-through) fraction was captured again with anti-CD81 MNPs and isolated on a magnetic column (**B**) or adsorbed on a CD81 coated ELISA plate (**C**). **A, B** : histograms of the flow analysis of captured (**A**) and re-captured (**B**) EVs. The numbers of events acquired in the same volume (9.7 μl) as evaluated with AccuCheck are shown. **C** : ELISA measurement of CD81 in the total EVs population (input) and in the fraction non-captured with anti-CD81 MNPs (flow-through). Note that the fraction not captured in the first run constitutes less than 1% of the originally captured EVs as evaluated with flow cytometry and about 6% as evaluated by ELISA. A representative experiment out of two to three is shown.

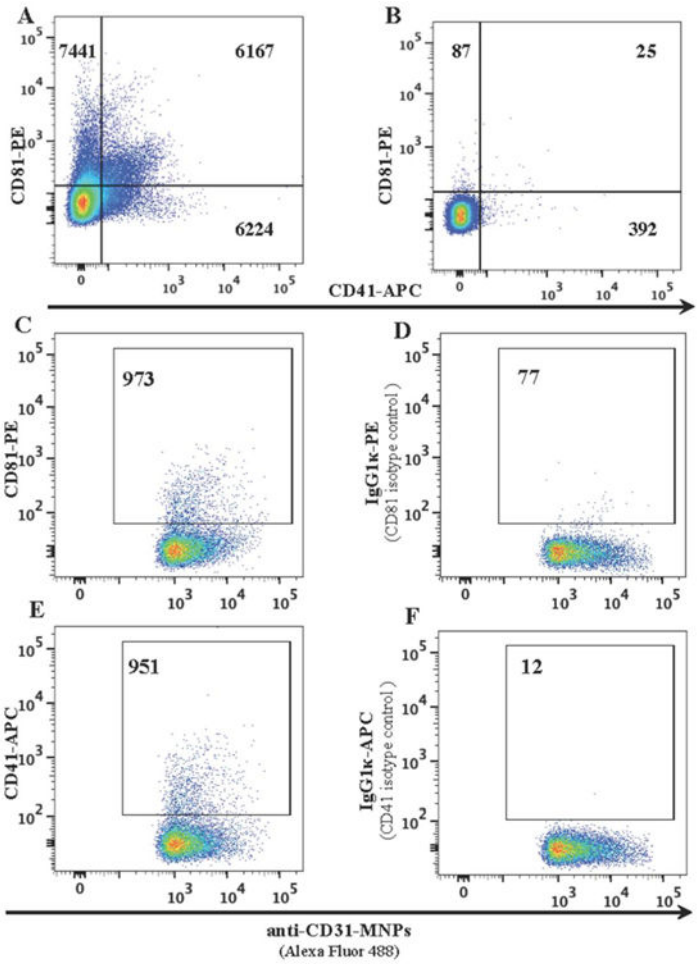

Figure 3. Specificity of capture and staining of plasma EVs

EVs isolated from platelet poor plasma were incubated with anti-CD31 MNPs (**A**) or with MNPs coupled to irrelevant antibodies (**B**) and stained with anti-CD81 PE and anti-CD41 APC antibodies. EVs captured with anti-CD31 MNPs were stained with either anti-CD81 PE (**C**) or anti-CD41APC antibodies (**E**), or stained with labeled isotype control PE mouse IgG1κ (**D**) and APC mouse IgG1κ (**F**) antibodies. Presented are the numbers of events acquired in the same volume (10 μl) as evaluated with AccuCheck. One representative experiment out of four (**A**, **B**) and one out of five (**C**, **D**) are shown. Note the specificity of both capture with MNPs bound to specific antibodies compared to capture with MNPs bound to isotype control antibodies (**A** vs. **B**), and the specificity of staining of captured EVs with specific antibodies compared to isotype control antibodies (**C** vs. **D** and **E** vs. **F**).

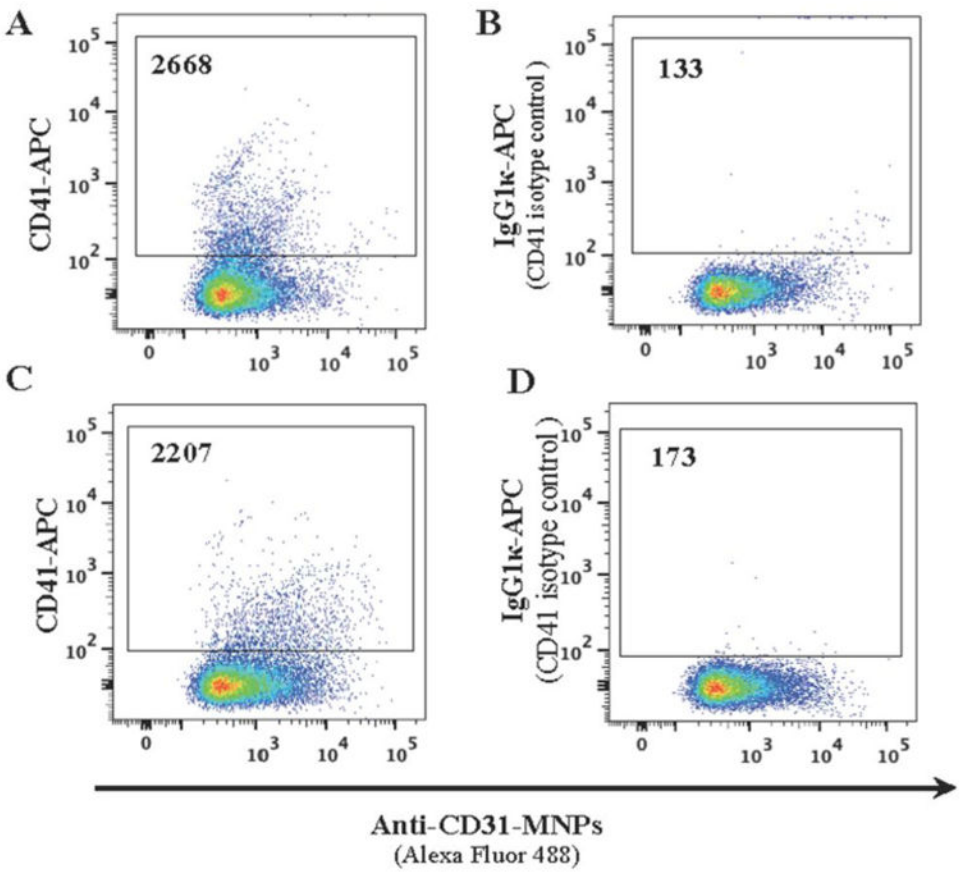

Figure 4. The lack of steric hindrance between MNPs and free antibodies

EVs isolated from platelet poor plasma were separated into two fractions. One fraction was captured with anti-CD31 MNPs labeled with Alexa Fluor 488 and stained with anti-CD41 APC-labeled antibody **(A);** the other was first stained for CD41 with the same antibody and then captured with anti-CD31 MNPs **(C).** Isotype controls: **B, D**. Presented are the numbers of events acquired in the same volume as evaluated with AccuCheck. A representative experiment out of two.

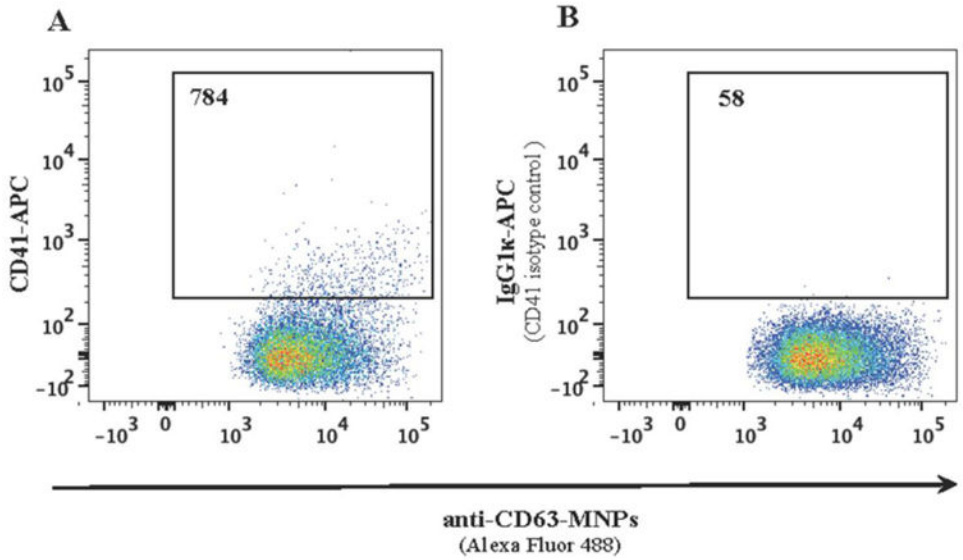

Figure 5. Direct analysis of blood plasma EVs

Concentrated platelet poor plasma was incubated with anti-CD63 MNPs. Captured EVs were stained with APC-labeled anti-CD41 antibodies (**A**) or with isotype control APC mouse IgG1κ (**B**), purified in a magnetic field and analyzed with flow cytometer. Presented are the numbers of events acquired in the same volume (9.7 μl) as evaluated with AccuCheck. A representative experiment of triplicates sets on platelet poor plasma from two donors is shown.